Structural determination of a W(001)$c(2\times2)$-Ag surface by x-ray photoelectron diffraction with multiple-scattering analysis

X. Chen and T. Abukawa
Research Institute for Scientific Measurements, Tohoku University, Sendai 980-77, Japan

J. Tani
Institute of Fluid Science, Tohoku University, Sendai 980-77, Japan

S. Kono
Research Institute for Scientific Measurements, Tohoku University, Sendai 980-77, Japan

(Received 26 May 1995)

We have studied x-ray photoelectron diffraction (XPD) for Ag 3*d* emission from the W(001)$c(2\times2)$-Ag surface with both full multiple-scattering cluster (MSC) and single-scattering cluster analyses. Quantitative structural parameters are obtained for the top layer of the Ag-W alloy structure. Systematic reliability factor searches based on MSC have shown that the outermost layer of the W(001)$c(2\times2)$-Ag surface forms a rumpled Ag-W alloy structure, and the plane containing Ag atoms is 0.3 ± 0.1 Å higher than the tungsten top layer. It has also been found that, in this system, there is a strong multiple-scattering effect in the photoelectron diffraction even for a high kinetic energy of 1115 eV, where single-scattering theory was generally assumed to be valid. This indicates that, for high Z and closely packed systems, the kinematical method is not suitable for the quantitative analysis of XPD experiments.

I. INTRODUCTION

The W(001) surface is a prototypical transition-metal surface, which plays the same role as Si does for the semiconductor surfaces. The interest in catalytic properties of noble metals on tungsten surfaces has been attracting much attention, and many surface techniques and theoretical methods have been carried out to study this system. It has been known that a clean W(001) surface undergoes a phase transition at around 200 K to a $c(2\times2)$ structure, the electronic and atomic structures of which have been studied by various techniques.[1–5] However, the understanding of noble metals (such as Cu, Ag, and Au) on the W(001) surface, where a similar $c(2\times2)$ phase is formed at one-half monolayer of adsorbate, is far from complete. Although the noble-metal/W(001) surface is known to form a surface alloy structure, as has been studied by ion scattering spectroscopy (ISS),[6–8] low-energy electron diffraction,[6,8] Auger electron spectroscopy,[6] thermal desorption spectroscopy,[9] and x-ray photoelectron diffraction (XPD),[10] no conclusive results regarding the details of atomic arrangement for the surface alloy structure have yet been found. The structural parameters for this $c(2\times2)$ surface may include lateral and vertical shifts of noble-metal adsorbates relative to the tungsten atoms in the top layer on the surface.

The aim of this work is to determine the atomic structure of the W(001)$c(2\times2)$-Ag surface [hereafter referred to as $c(2\times2)$-Ag] by the XPD technique with a full dynamical method. It is a significant expansion over the previous XPD study on this surface[10] with a kinematical theory, where no quantitative results related to the details of this surface alloy structure were obtained. Furthermore, our dynamical and kinematical studies have shown that, even for kinetic energy of 1115 eV, there is still a strong multiple-scattering effect on XPD from this surface, and it leads to a significant breakdown of single-scattering theory.

II. EXPERIMENT AND THEORY

The experiment of XPD for the Ag 3*d* core level from the $c(2\times2)$-Ag surface studied in this work was conducted in our early work.[10] A brief description of the experiment is as follows: as excited by an Al $K\alpha$ radiation source with a photon energy of 1486.6 eV, azimuthal scans of XPD patterns from the $c(2\times2)$-Ag surface were measured for Ag 3*d* emission at a grazing takeoff angle range of 6°–20°. The photoelectron diffraction experiment was performed by keeping the electron emission direction (to the detector) with respect to the sample surface at a constant takeoff angle θ_t, and rotating the sample about its normal to scan the Ag 3*d* photoelectrons as a function of azimuthal angle ϕ. During the scans, the angle between the incident x-ray beam and the electron emission direction is fixed at 75°. Details of the sample preparation and XPD experiment can be found in Ref. 10.

The full multiple-scattering cluster (MSC) scheme used in this study is an accurate and efficient concentric-shell algorithm (CSA).[11] In this scheme, we make use of the short inelastic scattering length of the electrons in a solid, where the electron multiple-scattering process is restricted to within a cluster of atoms centered at a silver emitter. A cluster of atoms including Ag and W is divided into a series of concentric shells to enable efficient

0163-1829/95/52(16)/12380(6)/$06.00

multiple-scattering evaluation at high speed with less computer memory. All the interatom propagation of the electrons is represented by the Green's functions, which relate the amplitudes of a spherical-wave expansion of the wave field about a particular atom to those of the same wave field about another, and the recursive relations[12] are intensively used to speed up the calculation. Similar efficient separable Green's-functions methods have been employed by other groups.[13,14] But the number of atoms M in a cluster becomes a limiting factor when photoelectron energy is high, roughly speaking ~ 1000 eV, where a larger cluster has to be implemented due to the increase in the electron mean free path. This makes it difficult to carry out MSC calculations due to M^3 scaling in computational time.[15] For computational convenience and efficiency, dividing the cluster into a series of concentric shells will significantly reduce the number of atoms in a shell to avoid the M^3 scaling, thus making the MSC calculation for a large cluster at high kinetic energy possible.

Another advantage of this scheme is that it can make use of the atoms' forward-scattering features in a concentric-shell geometry. In such a geometry, one can exploit the forward-scattering feature by (1) neglecting the intrashell multiple scattering due to a large scattering angle between atoms and electron emission directions, and (2) assuming that an outgoing traveling spherical wave incident on an atomic cluster shell has a negligible backward-scattered component. This forward-scattering approximation in the CSA scheme has been tested and compared with the result obtained by a full multiple-scattering calculation, and it was found that there is no essential difference between these two calculations at the kinetic energy of 1115 eV. This approximation results in speeding up the calculation for an order of magnitude in CPU time. In our CSA programs, the final states of the photoelectron with angular momenta of p and f due to a dipole emission from Ag $3d$ core levels are incorporated precisely, allowing the interference among photoelectron final states if they originate from the same core-level states.

In order to have a better comparison between the experimental and theoretical results, we have used the reliability factor (R factor) method for systematically analyzing the experimental XPD data for all possible surface models. For each azimuthal curve, both the experimental and theoretical XPD intensities were renormalized as

$$\xi(\theta_t,\phi)=\{I(\theta_t,\phi)-I_{\min}(\theta_t)\}/\{I_{\max}(\theta_t)-I_{\min}(\theta_t)\}\ , \tag{1}$$

where $I(\theta_t,\phi)$ is the XPD intensity; $I_{\min}(\theta_t)$ and $I_{\max}(\theta_t)$ are the minimum and maximum intensities for the azimuthal scan at θ_t. In the above definition, the value of $\xi(\theta_t,\phi)$ runs from 0 to 1. Our R factor is defined as

$$R=\sum_{N\theta_t}\eta(\theta_t)\sum_{N\phi}|\xi_{\text{expt}}(\theta_t,\phi)-\xi_{\text{calc}}(\theta_t,\phi)|/N_{\text{total}}\times100\%\ , \tag{2}$$

where $\xi_{\text{expt}}(\theta_t,\phi)$ and $\xi_{\text{calc}}(\theta_t,\phi)$ are the renormalized intensities for the experiment and theory, respectively, $\eta(\theta_t)$ is a weighting factor, the summations go over all the azimuthal scans ($N_{\theta t}$) and the data points (N_ϕ) in each scan, and N_{total} is the total number of data points. The advantages of such a definition of the R factor are that (1) R will not be affected adversely by the presence of a background (assumed to be smooth for each azimuthal scan) in the experiment, and (2) R will tune sensitively to the interference fine structure in the diffraction pattern. $\eta(\theta_t)$'s are used to compensate for curves with large anisotropies at the lower takeoff region. We have noticed that such a definition of the R factor is similar to that used by Bullock *et al.*[16] but with some differences.

III. MODELS FOR THE W(001)$c(2\times2)$-Ag SURFACE

In previous studies on the $c(2\times2)$-Ag surface, a surface alloy structure was highly favored by ISS (Refs. 6–8) and XPD.[10] Although it is still unclear what exact arrangement of Ag and W atoms in the alloy layer is formed, we can narrow down the possible surface models from general features of XPD patterns before starting the systematical R-factor search for the correct model with a full dynamical analysis.

Firstly, we have observed from the XPS patterns that the anisotropies are found to be very small above the takeoff angle of 20°, and no forward-scattering features are presented in the range of 6°–20° azimuthal scans. This allows us to eliminate immediately the models that include scatterers of either Ag or W well above the Ag emitters. Since the Ag coverage on this surface is one-half monolayer, this leads to a unique selection of one silver atom in the $c(2\times2)$ cell, but the number of tungsten atoms in the cell could be one for a surface alloy model or zero for an overlayer model.[10] One of the surface alloy models studied in this work is shown in Fig. 1, where a unit cell of $c(2\times2)$ is represented by a square. Since Ag emitters are in the outer layer of this structure, as explained above, the XPD pattern is most sensitive to the atomic arrangement in the top layers due to the forward-scattering feature of the atoms at high energy. This argument has further been supported by multiple-scattering calculations for models with or without subsurface W atoms, and it shows that the difference between the two simulations is trivial and within $\sim1\%$ of the R factor. Thus, we may choose models including only top Ag and W layers, where the Ag-W layer spacing can be different in height by ΔZ as defined in Fig. 1. It is obviously seen in the figure that, if the tungsten atoms in the top layer are moved down considerably, atoms in the surface unit cell are then reduced to one Ag atom per cell; this is known as an overlayer model.

Secondly, from a simple classical hard-sphere model, considering the atomic radii of Ag and W (1.45 and 1.37 Å, respectively) and the lateral space available for a surface unit cell (6.32 Å$\times$6.32 Å), the silver and tungsten atoms have to be at positions close to the fourfold sites of the unreconstructed W(001) surface. Taking the W atom position as a reference, the in-plane displacement for the

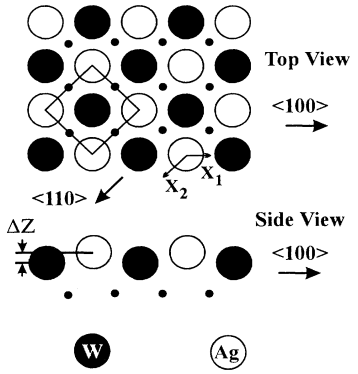

FIG. 1. Top and side views of a rumpled surface alloy structure for the W(001)$c(2\times2)$-Ag surface. A square in the top view shows a $c(2\times2)$ unit cell on the surface. Shaded and open circles represent tungsten and silver atoms, respectively. Small solid dots are tungsten atoms in bulk positions. ΔZ is defined as Ag-W interlayer spacing.

Ag atom should be small due to the constraints of Ag-W bond lengths, however, the vertical movement for Ag can be significant in such an alloy structure.

In the following dynamical analysis, we carry out MSC calculations for the surface alloy model, as shown in Fig. 1, and perform systematic R-factor analyses to optimize the surface-structure parameters with the XPD experiment.

IV. DYNAMICAL ANALYSIS

In our dynamical simulations of XPD from the $c(2\times2)$Ag surface, the kinetic energy of the photoelectron is set to be 1115 eV in vacuum. The scattering phase shifts for Ag and W were calculated within a muffin-tin potential approximation using atomic wave functions of Ag and W from a Hermann-Skillman program.[17] The temperature effect of the lattice vibration was also considered by using temperature-dependent phase shifts[18] for both Ag and W. The Debye temperatures of 225 and 400 K are chosen for Ag and W.[19] The use of bulk Debye temperatures does not affect the quantitative conclusion of this study. The angular momenta of the scattering phase shifts at room temperature of up to $L_{max}=20$ were chosen for both Ag and W atoms. The number of partial waves (L_{out}) in the scattering matrix **S** was set to 60.[11] The inner potential V_{in} is an adjustable parameter, and was finally set to 10 eV, which results in a best fit between the experiment and MSC calculation. Due to a dipole transition, the final states of the photoelectron from Ag $3d$ emission are in p- and f-wave forms. The radial matrix elements and the corresponding phase shifts for the emitted waves are calculated by a MUFPOT program, and they are 0.00419 bohr and 5.636 rad for p wave ($l=1$), and 0.0227 bohr and 2.704 rad for f wave ($l=3$), respectively.

Due to the surface sensitivity of XPD at grazing regime for this energy range, MSC simulations were performed on clusters involving only one silver and tungsten layer for the surface alloy models, as shown in Fig. 1. The electron mean free path is 20 Å according to the universal curve.[20] The size of the cluster is therefore chosen to be 25 Å in radius for a full convergence, and it includes about 200 Ag and W atoms. A series of MSC simulations were first carried out for the alloy structures with Ag and W atoms at the fourfold sites of the unreconstructed W(001) surface but with various values of Ag-W layer spacing, ΔZ. The R factors were evaluated by Eqs. (1) and (2) for each ΔZ, and the resulting R-ΔZ curve is plotted in Fig. 2 (a solid line with open squares). It is clearly seen from the R-ΔZ curve that the best agreement between MSC calculations and the experiment has been reached at $\Delta Z=0.3$ Å, where a minimum of $R=14.1\%$ is obtained. It is noticed here that a $\Delta Z=0.3$ Å structure refers to a rumpled ally surface with a silver layer locating 0.3 Å higher than the tungsten one. In the same figure, the $\Delta Z=-0.2$ Å end refers to a model where Ag emitters are under the W layer by 0.2 Å, and the $\Delta Z>1.8$ Å one approaches the limit of overlayer structure. We have shown in Fig. 3 the azimuthal plots of experimental XPD (dotted lines) and MSC for the optimized structure of $\Delta Z=0.3$ Å (solid lines). It is seen that the MSC curves match the experimental ones fairly well for most of the azimuthal plots.

Although good agreement between the experiment and MSC has been achieved for the rumpled alloy structure where the positions of Ag adsorbates are at the fourfold sites of the unreconstructed W(001) surface, a possible in-plane shift of Ag atom away from its highly symmetric position will be investigated next. But such a shift should

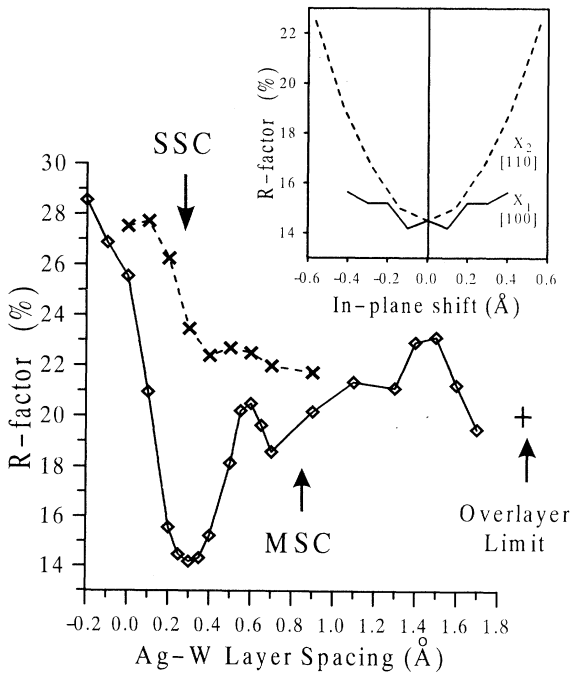

FIG. 2. R factor vs Ag-W interlayer spacing (ΔZ) for MSC (solid line with open squares) and SSC (dashed line with crosses). Inset shows the R factors vs in-plane shifts of Ag atom along [100] (solid line) and [110] (dashed line) for MSC.

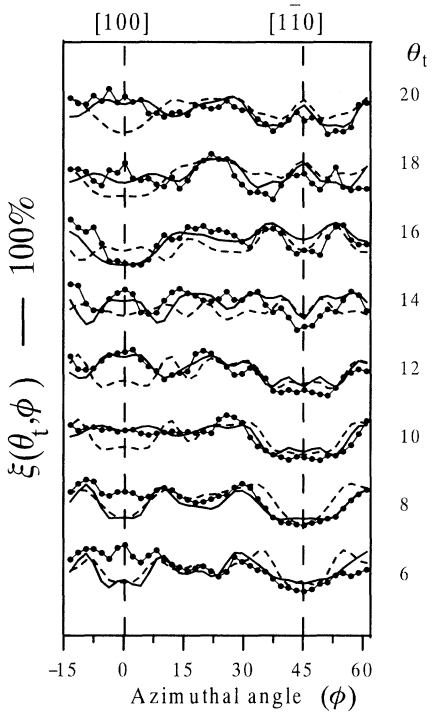

FIG. 3. Azimuthal scans of 3d XPD experiment (dotted lines), MSC (solid lines), and SSC (dashed lines) with a rumpled alloy structure of $\Delta Z=0.3$ Å.

be small and within a few-tenths of an angstrom (0.34 Å along [100] and 0.51 Å along [110]) due to the constraints of Ag-W bond lengths for the alloy surface of $\Delta Z=0.3$ Å. Thus, we performed MSC simulations with models including different lateral shifts of the Ag atom off its fourfold symmetric point. The assumed in-plane shifts of Ag adsorbates are along the [100] and [110] directions by X_1 and X_2, respectively, as shown on Fig. 1. The resulting R-X_1 and R-X_2 curves for MSC are shown in the inset of Fig. 2 with solid and dashed lines, respectively. It can be seen from R-X_1 and R-X_2 that the R factor is sensitive to the change of Ag atom position along [110] direction but not so along the [100] direction. Such behaviors of the R factor can be explained by the fact that, at high kinetic energy, diffraction patterns are dominated by the forward-scattering peaks (mainly their first-order diffraction peaks at grazing regime in the experiment), and are most sensitive to the local geometry around an emitter. Since W atoms are almost in the same plane as Ag adsorbates, Ag-Ag scattering along [110] and Ag-W scattering along [100] will dominate the diffraction and produce the most prominent features in the patterns. However, the Ag-Ag scattering remains the same for both direction and magnitude due to a $c(2\times2)$ periodicity. But the diffraction features due to the nearest-neighbor Ag-W scattering will be affected depending on the movement of the silver atom. Namely, the moving silver atom along the [100] direction will result in only changing in emitter-scatterer distance, which will not affect the forward-scattering feature very much; however, shifting the silver atom along [110] will cause the forward-scattering peak of Ag-W to scatter off its [100] direction, and hence change the pattern considerably. The insensitivity of the R factor to the movement of Ag along [100] is a drawback for the XPD technique in this high-energy range. But we may still conclude that the interlayer spacing between the Ag and W layers is 0.3 ± 0.1 Å and the lateral shift of the Ag atom off its fourfold site along the [110] direction is within 0.2 Å. Further XPD studies on a possible in-plane shift of Ag atom along [100] are needed to be carried out at a lower kinetic energy range, where the diffraction pattern contains more structural information about local geometry.

V. FAILURE OF KINEMATICAL THEORY

Kinematical analysis has also been performed in this work to check the effect of the multiple scattering on the XPD from this surface. Single-scattering cluster (SSC) simulations were carried out by the same CSA programs, where multiple-scattering channels were switched off, but with the same input control parameters, e.g., the size of clusters, scattering phase shifts, and number of partial waves for the scattering matrix, etc. It is noted that in order to have an equivalent comparison between the kinematical and dynamical theories, discrepancies caused by different theoretical approaches and approximations made by different algorithms or programs can be eliminated in this way.

The surface models used for the SSC simulations are chosen near the rumpled alloy structure optimized by MSC analysis. R factors were calculated as a function of Ag-W layer spacing in the range of $\Delta Z=0$–0.9 Å with Ag and W atoms at the fourfold sites of the unreconstructed W(001) surface. The R-ΔZ curve is shown by a dashed line with crosses in Fig. 2. It is seen that the R factors for SSC are in the range of 21–28%, which is significantly higher than the optimized $R=14.1\%$ obtained by MSC. It is evident that there is no indication of any possible favored structures in this region from the kinematical analysis. We have also shown the azimuthal scans of SSC for the rumpled alloy surface of $\Delta Z=0.3$ Å in Fig. 3 by dashed lines. It is obviously seen from the figure that agreement between the experiment and SSC is poor for most of the azimuthal scans, indicating the failure of the kinematical theory and the dynamical process to play an important role in this system.

In order to have a better view of the diffraction features of the experiment and theories, diffraction intensities of experiment, and theories of MSC and SSC for the rumpled alloy structure of $\Delta Z=0.3$ Å, are shown in stereographic projection with a thermal scale in Fig. 4. In an effort to get a closer look at the experiment and the theories, the experimental XPD was plotted on the left-hand side of the projection with a mirror symmetry of the theoretical one. To emphasize the grazing takeoff angle regions, where the experimental XPD data were taken, the takeoff angle is scaled with a formula of $r=r_0[1-\sin(\theta_t)]$, where r is the radius from the center and r_0 the full scale radius at $\theta_t=0°$. The major

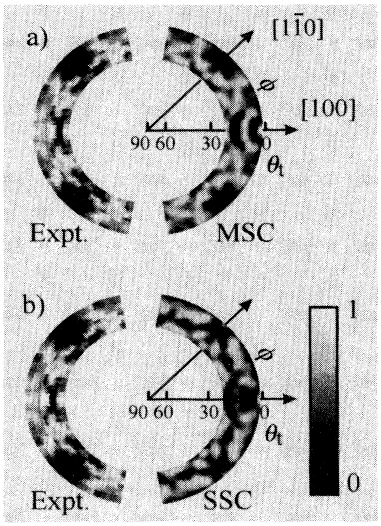

FIG. 4. Stereographic projections of Ag 3d XPD intensities from the W(001)$c(2\times2)$-Ag surface. The renormalized intensities are shown on (a) $\xi_{\rm expt}(\theta_t,\phi)$ and $\xi_{\rm MSC}(\theta_t,\phi)$, and (b) $\xi_{\rm expt}(\theta_t,\phi)$ and $\xi_{\rm SSC}(\theta_t,\phi)$. The experimental XPD is plotted as a mirror symmetric pattern of the theoretical one. Both simulations incorporate the same rumpled alloy structure of $\Delta Z=0.3$ Å.

diffraction features in XPD experiment (mirror symmetry) are a group of peaks along the [100] direction, large dip along the [1$\bar{1}$0] direction, and a triangle-shaped pattern in between. By carefully comparing the theoretical patterns on the right side of the figures with the experimental one on the left, it can be seen that most of these diffraction features of peaks and dips and their positions are reproduced well by the MSC pattern, whereas it is not so for the SSC one.

VI. DISCUSSION AND CONCLUSIONS

A comparison between azimuthal scans of MSC and that of SSC in Fig. 3 has shown that there are significant differences between the curves of MSC and SSC in the takeoff angle range of 6°–20°. Our recent kinematical and dynamical studies on XPD from Si(111) $\sqrt{3}\times\sqrt{3}$-Ag and -Sb surfaces[21] have shown that SSC tends to hold on at higher takeoff angles above 12°. In other words, SSC fails at the low takeoff angle region for both cases. It seems that the multiple-scattering effect on XPD from the $c(2\times2)$-Ag surface is more prominent than that from the $\sqrt{3}\times\sqrt{3}$ surfaces. In order to justify the above assumption, we have further carried out MSC and SSC simulations from the $c(2\times2)$-Ag surface for higher takeoff angles of up to 50° (the anisotropies at these high takeoff angles are small in reality). It was found that at takeoff angle of above 28°, the curves of SSC match well with that of MSC, contrary to the large differences at lower takeoff angles ($<28°$) between the two theories.

It is well known that at high kinetic energy range where diffraction features are dominated by the forward-scattering peaks of the scatterers, the single-scattering theory is generally believed to be valid, but it fails along or close to closely packed directions, where multiple scattering plays an essential role. For closely packed monolayer systems, such as the $c(2\times2)$-Ag surface, where emitters are located at the outermost layer of the surface, there are no such dominated forward-scattering peaks appearing in the pattern. A dynamical process could still play an important role at the grazing regime, where scatterers are closely packed. On the other hand, at the higher takeoff angle range, it is farther away from the closely packed region and therefore the multiple-scattering effect becomes insignificant. But the critical takeoff angle θ_c, which is the smallest angle possible for a kinematical theory to still be valid, may differ from system to system, and even be a function of kinetic energy of electrons. We have found that $\theta_c=28°$ for the $c(2\times2)$-Ag surface with a surface atomic density of ~10 atoms/nm^2, and $\theta_c=12°$ for $\sqrt{3}\times\sqrt{3}$-Ag and -Sb surfaces[21] with a density of ~5 atoms/nm^2. We may conclude that, in general, θ_c increases with increasing surface atomic density and atomic number Z.

In summary, XPD data for Ag 3d emission from the W(001)$c(2\times2)$-Ag surface have been analyzed by a dynamical analysis using a concentric-shell algorithm. In such a scheme, a multiple-scattering calculation can be performed on sufficiently large clusters (25 Å in radius) at a kinetic energy of 1115 eV. Quantitative structural results for a rumpled surface alloy structure for the W(001)$c(2\times2)$-Ag surface have been obtained. The dynamical analysis has shown that, for this surface, the Ag layer is 0.3 ± 0.1 Å higher than the W top layer. It is also found that there is a strong multiple-scattering effect on the photoelectron diffraction, even at a kinetic energy of 1115 eV, where single-scattering theory was usually assumed to be valid. It has been demonstrated by this study that kinematical theory is not suitable for the quantitative study on XPD from this high Z and closely packed system.

[1]D. A. King, Phys. Scr. **T4**, 34 (1983), and references therein.
[2]L. F. Matheiss and D. R. Hamann, Phys. Rev. B **29**, 5372 (1994).
[3]C. L. Fu, A. J. Freeman, E. Wimmer, and M. Weinert, Phys. Rev. Lett. **54**, 2261 (1985).
[4]M. S. Altman, P. J. Estrup, and I. K. Robinson, Phys. Rev. B **38**, 5211 (1988).
[5]G. S. Elliott, K. E. Smith, and S. D. Kevan, Phys. Rev. B **44**, 10 826 (1991).
[6]G. A. Attard and D. A. King, Surf. Sci. **188**, 589 (1987).
[7]G. A. Attard and D. A. King, Surf. Sci. **222**, 360 (1989).
[8]S. H. Overbury and D. R. Mullins, J. Vac. Sci. Technol. A **7**, 1942 (1989).
[9]G. A. Attard and D. A. King, Surf. Sci. **223**, 1 (1989).
[10]H. Takahashi, M. Sasaki, S. Suzuki, S. Sato, T. Abukawa, S. Kono, and J. Osterwalder, Surf. Sci. **304**, 65 (1994).

[11]D. K. Saldin, G. R. Harp, and X. Chen, Phys. Rev. B **48**, 8234 (1993).
[12]V. Fritzsche, J. Phys. Condens. Matter **2**, 9735 (1990).
[13]J. J. Barton and D. A. Shirley, Phys. Rev. B **32**, 1906 (1985).
[14]D. Friedman and C. S. Fadley, J. Electron. Spectrosc. Relat. Phenom. **51**, 689 (1990).
[15]J. B. Pendry, in *Determination of Surface Structure by LEED,* edited by P. M. Marcus and F. Jona (Plenum, New York, 1984), p. 3.
[16]E. L. Bullock, G. S. Herman, M. Yamada, D. J. Friedman, and C. S. Fadley, Phys. Rev. B **41**, 1703 (1990).
[17]F. Herman and S. Skillman, *Atomic Structure Calculation* (Prentice Hall, Englewood Cliffs, NJ, 1963).
[18]J. B. Pendry, *Low Energy Electron Diffraction* (Academic, London, 1974).
[19]C. Kittel, *Introduction to Solid State Physics* (Wiley, New York, 1986).
[20]M. P. Seah and W. A. Dench, Surf. Interface Anal. **1**, 2 (1979).
[21]X. Chen, T. Abukawa, and S. Kono (unpublished).

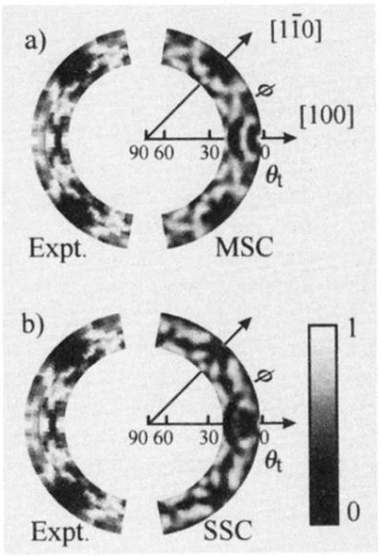

FIG. 4. Stereographic projections of Ag 3*d* XPD intensities from the W(001)$c(2\times2)$-Ag surface. The renormalized intensities are shown on (a) $\xi_{\text{expt}}(\theta_t,\phi)$ and $\xi_{\text{MSC}}(\theta_t,\phi)$, and (b) $\xi_{\text{expt}}(\theta_t,\phi)$ and $\xi_{\text{SSC}}(\theta_t,\phi)$. The experimental XPD is plotted as a mirror symmetric pattern of the theoretical one. Both simulations incorporate the same rumpled alloy structure of $\Delta Z=0.3$ Å.